Radiation-induced amorphization of ordered intermetallic compounds CuTi, $CuTi_2$, and Cu_4Ti_3: A molecular-dynamics study

Michael J. Sabochick
Department of Engineering Physics, Air Force Institute of Technology, Wright-Patterson Air Force Base, Ohio 45433

Nghi Q. Lam
Materials Science Division, Argonne National Laboratory, Argonne, Illinois 60439
(Received 6 August 1990; revised manuscript received 18 January 1991)

Solid-state amorphization resulting from the introduction of chemical disorder and point defects in the ordered intermetallic compounds CuTi, $CuTi_2$, and Cu_4Ti_3 was investigated, with use of the isobaric-isothermal molecular-dynamics method in conjunction with embedded-atom potentials. Antisite defects were produced by randomly exchanging Cu and Ti atoms, and vacancies and interstitials were created by removing atoms at random from their normal sites and inserting atoms at random positions in the lattice, respectively. The potential energy, volume expansion, and pair-correlation function were calculated as functions of the numbers of atom exchanges and point defects. The results indicated that, although both chemical disordering and point-defect introduction increased the system energy and volume, the presence of point defects was essential to trigger the crystalline-to-amorphous transition. By comparing the pair-correlation function calculated after the introduction of point defects with that of the quenched liquid alloy, the critical damage dose (in dpa, displacements per atom) for amorphization was estimated for each compound: ~ 0.7 dpa for CuTi, ~ 0.5 dpa for $CuTi_2$, and ~ 0.6 dpa for Cu_4Ti_3. At the onset of amorphization, the volume expansions were found to be $\sim 1.9\%$, $\sim 3.7\%$, and $\sim 1.7\%$ for these respective compounds. In general, the results obtained in the present work are in good agreement with experimental observations.

I. INTRODUCTION

It has been known for some time that a number of crystalline materials can be rendered amorphous by irradiation at low temperatures.[1–4] The amorphous phase was observed in ion-implanted alloys, ion-mixed thin films, and regions irradiated by energetic electrons inside a high-voltage electron microscope. The tendency of a metallic alloy towards amorphization during irradiation has been correlated with its narrow compositional range,[5] the difference in crystal structure of the alloy components,[6] the complex crystal structure of the alloy in the unirradiated state,[3] the position of the alloying elements in the periodic table,[3,7] and the high-ordering energy of the compound.[3] Ultimately, however, the physical basis for the destabilization of the irradiated crystalline phase is related to an increase in the free energy induced by irradiation. Such an energy increase can be stored in the lattice in the form of severe chemical disorder[3,8–10] or high defect concentrations.[2,11–16]

In experiments, the degree of chemical disorder is characterized by measuring the Bragg-Williams long-range order parameter S, which has values between 1 and 0, corresponding to the perfectly ordered and random states of the alloy, respectively. Luzzi *et al.*[3,8–10] measured the minimum value of S, $S_{\min}$, achievable during electron irradiation at various temperatures and found a sharp increase in $S_{\min}$ around 270 K in the intermetallic compounds $CuTi_2$ (Ref. 9) and Cu_4Ti_3.[3,8,10] Below this critical temperature, significant chemical disorder was observed during irradiation, whereas above this temperature the attainable degree of chemical disordering was drastically reduced and secondary defects were created in the sample. The critical temperature for chemical disordering was found to coincide with that for amorphization. These observations led Luzzi *et al.* to suggest that chemical disordering plays a major role as an energy storage mechanism prior to the crystalline-to-amorphous (c-a) transition.[3,8–10] Recently, amorphization by the introduction of chemical disorder was also simulated by Massobrio, Pontikis, and Martin[17] using molecular dynamics in conjunction with a tight-binding potential derived for the crystalline compound $NiZr_2$. The pair-distribution functions $g(r)$ were calculated for various long-range order parameters. Based on the response of $g(r)$ to changes in S, Massobrio, Pontikis, and Martin[17] concluded that amorphization occurred when S decreased to values less than or approximately equal to 0.6.

In many other studies, however, point-defect models have been proposed, based on the concept that the primary mode of energy storage arises from the accumulation of point defects.[2,11–16] The idea that the material becomes amorphous when the defect concentration exceeds a critical value was first advanced by Swanson, Parsons, and Hoelke.[18] They estimated a critical concentration of approximately 0.02–0.04 site fraction. Mori, Fujita, and Fujita[11] observed that amorphous zones were formed as small islands along dislocation lines in electron-irradiated NiTi. Arguing that, since interstitials preferentially annihilate at dislocations, enrichment of vacancies occurs in the regions surrounding dislocations, Mori, Fujita, and Fujita suggested a model for the c-a

transition based on the accumulation of vacancies exceeding a critical concentration. Limoge and Barbu,[12] on the other hand, emphasized the importance of interstitials in the amorphization process, pointing out that in some ordered compounds, like FeAl and NiAl, very high concentrations of structural vacancies exist, but only cause deviations from stoichiometry, not amorphization. These authors attributed the existence of a critical temperature for amorphization to the onset of migration of interstitials whose mobility was reported to be significantly reduced in many alloys.[19–22] Subsequently, Simonen[23] modeled the amorphization kinetics in NiTi under electron irradiation and found that an interstitial migration energy of approximately 1.0 eV was necessary in order to rationalize the observed *c-a* transition. Another point-defect model was proposed by Pedraza,[2] based on the formation of strongly bound vacancy-interstitial complexes which are stabilized by short-range chemical ordering. Model calculations performed by Pedraza for the kinetics of amorphization in NiTi indicated that good agreement with experiment was obtained if the complex binding energy was between 0.7 and 1.0 eV. Finally, in a recent study of electron irradiation-induced *c-a* transition of precipitates in Zircaloy, Motta, Olander, and Machiels[24] used a kinetic model that includes the contributions of both chemical disordering and accumulation of point defects (mainly vacancies) and found that these contributions were equivalent. Also, with reasonable choice of physical parameters for point-defect and ordering energies, the temperature and dose rate dependence of the critical dose for amorphization could be explained by model calculations.

Amorphization induced by electron irradiation represents the simplest case of *c-a* transitions to study, both experimentally and theoretically, because only Frenkel pairs are involved; concepts like thermal spike, local melting, or quenching can be safely excluded. Despite this simplicity, however, there is a drawback in the experimental investigation, since it is difficult to unambiguously determine which mechanism, chemical disordering or point-defect creation, is dominant in inducing amorphization. This is due to the fact that the incident electrons generate lattice defects which also result in chemical disorder and volume expansion, both of which are always observed to occur prior to the *c-a* transition. Because of this experimental drawback, several molecular-dynamics studies have been carried out in recent years. In computer simulations, one can easily induce chemical disorder or vary the system volume without introducing point defects, and thus the individual effects of these mechanisms can be determined. Unfortunately, due to the lack of appropriate interatomic potentials for alloys, most of these simulations have so far been performed on monatomic solids. In addition, the evidence to date from computer simulations is nevertheless conflicting. For example, studies of amorphization by the introduction of Frenkel pairs[15,25] and of interstitials alone[14,15] in pure fcc systems have suggested that point defects were sufficient to induce the *c-a* transition, even though it is known that pure fcc metals cannot be amorphized in the laboratory. Hsieh and Yip[26] simulated the effect of interstitial insertion on the destabilization of an A_3B ordered lattice with Lennard-Jones potentials and concluded that chemical disordering played a dominant role in the amorphization process, in agreement with the simulation result for $NiZr_2$ by Massobrio, Pontikis, and Martin.[17]

In the present work, molecular-dynamics simulations have been performed to study the mechanisms of radiation-induced amorphization in the three ordered compounds CuTi, $CuTi_2$, and Cu_4Ti_3, for which realistic interatomic potentials could be developed. The relative significance of chemical disordering and introduction of lattice defects in triggering the *c-a* transition was examined in detail. It is noted that, among the alloys investigated experimentally, the intermetallic compounds of the Cu-Ti system have been studied most systematically,[3] and it has been suggested that chemical disordering played a critical role in amorphization of these compounds.[3,8–10]

II. SIMULATION PROCEDURE

A. Molecular-dynamics model

The primary atomistic simulation technique used in the present work was an isothermal, isobaric molecular dynamics scheme modified from the computer code DYNAMO.[27] The model lattices are illustrated in Fig. 1. The model system that represents the γ-phase CuTi compound has a $B11$ structure and contains 576 atoms, equally divided between Cu and Ti. For the ordered compound $CuTi_2$, a microcrystallite of the $C15_b$ structure, containing 882 atoms, was used. The crystal structure of Cu_4Ti_3 is more complicated; it is a Frank-Kasper-type structure, consisting of seven stacked body-centered-tetragonal sublattices. The model lattice of Cu_4Ti_3 contains 504 atoms. The interactions between atoms in the system were governed by appropriate poten-

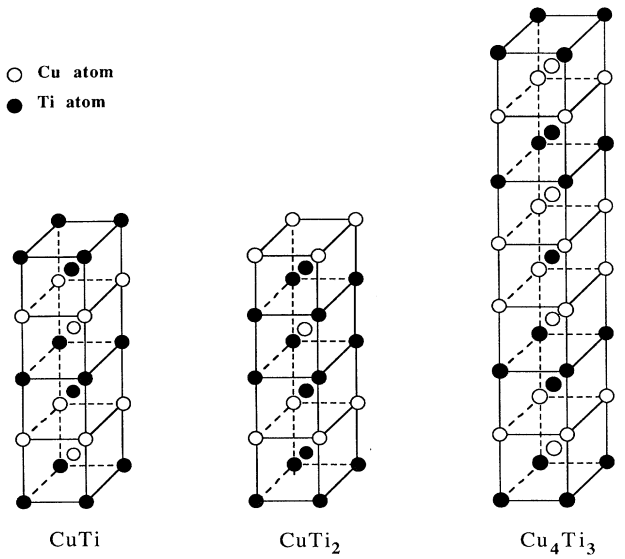

FIG. 1. Crystal structures of CuTi, $CuTi_2$, and Cu_4Ti_3.

tials, which we have developed on the basis of the embedded-atom method[28] (see below). The simulations were all performed at 160 K and at zero pressure.

The effect of chemical disordering on the structural stability of the system was investigated by switching atoms in the lattice. A perfect lattice was equilibrated for 5000 time steps ($\Delta t = 2\times10^{15}$ s) and then every 10 time steps, a random pair of Cu and Ti atoms was exchanged. The system configuration, defined by the system edge lengths and the atom positions and velocities, was periodically saved during the exchange process. The configurations were subsequently allowed to evolve for 6000 time steps, long enough for the volume and energy to reach equilibrium. To simulate the effect of Frenkel-pair generation, on the other hand, a randomly selected atom was removed (creating a vacancy) and then reinserted at a random position (forming an interstitial) every 10 time steps. To prevent high potential-energy configurations from excessively heating the system or causing numerical instabilities, the interstitial atom was inserted at least 1.5 Å from any other atom, and the system was partially relaxed using an efficient energy minimization scheme.[29] As with the atom exchange, the system configuration was also saved periodically and subsequently equilibrated for 6000 time steps in separate runs. The equilibrated systems were analyzed by comparing their volumes, total energies, atom-position projections, and pair-correlation functions $g(r)$ with those of the perfect lattice.

B. Interatomic potentials

The interatomic potentials for the Cu-Ti system were developed with the approach of Oh and Johnson,[30] which is based on the embedded-atom method (EAM).[28] The potential energy of a system of N atoms is given by

$$U(\mathbf{r}_1,\ldots,\mathbf{r}_N)=\sum_i F_k[\rho(\mathbf{r}_i)]+\sum_{i<j}\Phi_{km}(r_{ij}) , \quad (1)$$

where $\mathbf{r}_i$ is the position of atom i, $\rho(\mathbf{r}_i)$ is the electron density at atom i due other atoms in the system, F is the embedding function, Φ is the repulsive potential, and r_{ij} is the distance between atoms i and j. The subscripts k and m denote the species of atoms i and j, respectively. The electron density is given by

$$\rho(\mathbf{r}_i)=\sum_{j\neq i} f_m(r_{ij}) . \quad (2)$$

The functions Φ and f have the analytic forms

$$\Phi_{km}(r_{ij})=\Phi_{e,km}(r_{ij}/r_{e,km})^{-\gamma_{km}} \quad (3)$$

and

$$f_m(r_{ij})=f_{e,m}\exp[-\beta_m(r_{ij}/r_{e,mm}-1)] . \quad (4)$$

For computational convenience, Φ_{km} and f_m were truncated smoothly at the cutoff radii $r_{c,km}=s_{c,km}r_{e,km}$ and $r_{d,m}=s_{d,m}r_{e,mm}$, respectively, by defining an effective potential[31]

$$\Phi_{km}^{\text{eff}}(r)=\Phi_{km}(r)-\Phi_{km}(r_{c,km})+\frac{r_{c,km}}{N_c}[1-(r/r_{c,km})^{N_c}]\left.\frac{d\Phi_{km}}{dr}\right|_{r_{c,km}} \quad (5)$$

and an analogous function $f_m^{\text{eff}}(r)$. In all cases, $N_c=20$ was used.

The embedding function is chosen such that the equation of state formulated by Rose *et al.*[32] and modified by Oh and Johnson[30] is satisfied for the perfect lattice subject to compression or expansion. The embedding function is given by

$$F_k[\rho_k(z)]=E_k(z)-\sum_n \Phi_{kk}(zr_n) . \quad (6)$$

Here z is the ratio of the edge length of the expanded or compressed perfect lattice to that at zero pressure, and the electron density is now written as

$$\rho_k(z)=\sum_n f_k(zr_n) , \quad (7)$$

with the sum over n corresponding to the neighbors of an atom in the perfect lattice. The energy per atom $E_k(z)$ is[30]

$$E_k(z)=-E_{c,k}\left[1+\alpha_k(z-1)\left[\frac{1}{z^{h_k}}-\frac{h_k}{z}+h_k\right]\right]\times\exp[-\alpha_k(z-1)] , \quad (8)$$

with the cohesive energy $E_{c,k}$ and the constant α_k being given by Rose *et al.*[32] for particular elements, and h_k a "hardness" factor as described by Oh and Johnson.[30]

The fitting of the potential parameters consisted of two steps. In the first step, the pure metal properties of Cu and Ti were fitted, specifying the parameters $\Phi_{e,kk}$, γ_{kk}, $s_{c,kk}$, β_k, and $s_{d,k}$, where $k=1$ or 2 corresponding to Cu or Ti, respectively. These parameters are listed in Table I. It is noted that the parameter $f_{e,k}$ does not affect pure metal properties. For Cu, the properties fitted were the atomic volume Ω, bulk modulus B, shear modulus G, anisotropy ratio $A=2C_{44}/(C_{11}-C_{12})$, relaxed vacancy formation energy E_v^f, and vacancy migration energy E_v^m.

TABLE I. Parameters of the Cu, Ti, and CuTi potentials. Here $r_{e,km}$ is in nm, $\Phi_{e,km}$ and $E_{c,k}$ are in eV, and all other quantities are dimensionless.

Parameter	Cu $k=m=1$	Ti $k=m=2$	CuTi $k=1,\ m=2$
$r_{e,km}$	0.255 6	0.295	0.295
$\Phi_{e,km}$	0.845 746	0.293 049	0.453 404
γ_{km}	6.039 482	8.816 339	5.748 716
$s_{c,km}$	1.933	1.66	1.50
$f_e(\text{Cu})/f_e(\text{Ti})$			1.0
β_k	4.661 134	4.41	
$s_{d,k}$	1.933	1.66	
h_k	2.5	3.2	
$E_{c,k}$	3.54	4.85	
α_k	5.085	4.743	

TABLE II. Fitting results for pure Cu and Ti. Here Ω is expressed in Å^3; B, G, C_{11}, C_{12}, C_{13}, C_{33}, and C_{44} are in Mbar; and E_v^f and E_v^m are in eV.

	Cu			Ti		
Quantity	Experiment	Present work	Ref. 30	Experiment	Present work	Ref. 30
Ω	11.81[a]	11.81	11.81	17.64[a]	17.64	17.64
B	1.38[b]	1.38	1.38			
G	0.55[b]	0.59	0.55			
C/C'	3.19[b]	3.27	3.21			
C_{11}				1.761[a]	1.883	1.835
C_{12}				0.868[a]	0.768	0.78
C_{13}				0.683[a]	0.672	0.67
C_{33}				1.891[a]	1.918	1.992
C_{44}				0.508[a]	0.454	0.409
E_v^f	1.31[c]	1.27	1.31	1.55[d]	1.55	1.55
E_v^m	0.76[c]	0.71	~0.55			
c/a				1.587[e]	1.6113	1.6173

[a]Reference 38.
[b]Reference 39.
[c]Reference 40.
[d]Reference 41.
[e]Reference 42.

In the case of Ti, the atomic volume, the elastic constants, c/a, and the relaxed vacancy formation energy were fitted. The fitted parameters are shown in Table II. In general, the fit was quite good, with a maximum relative error of approximately 10%. In addition, the relative stabilities of fcc, hcp, and bcc structures were checked for both potentials, and it was found that the fcc and hcp structures were the most stable for Cu and Ti, respectively.

In the second step, the structure, the equilibrium atomic volume, and the heats of formation of CuTi and $CuTi_2$ were fitted. This step specified $f_{e,1}$, $\Phi_{e,12}$, γ_{12}, and $s_{c,12}$, whose values are given in Table I. The above properties of the compounds were fitted to within approximately 10% for CuTi, as shown in Table III. The fit to $CuTi_2$ was not quite as good, with deviations of approximately 15% between experimental and fitted values (Table III). It was found during the fitting that either compound could individually be fitted exactly, but that some compromise was necessary in order to achieve a simultaneous fit to both. No systematic fitting was performed for Cu_4Ti_3 since its heat of formation was not known. However, the potential derived for CuTi and $CuTi_2$ was also used for simulation of Cu_4Ti_3, because this potential stabilizes the structure and correctly predicts the lattice constants (a and c) for this compound. The calculated values of a, equilibrium atomic volume, and heat of formation of Cu_4Ti_3 are tabulated in Table III.

III. RESULTS AND DISCUSSION

A. Amorphization of CuTi

The changes in the system volume and potential energy as a result of random atom exchanges are shown in Fig. 2. As the number of exchanges was increased, the system volume smoothly increased to a value approximately 1.7% larger than that of the perfect lattice, and then decreased slightly. Similarly, the energy rapidly increased to a maximum level before slowly decreasing to a value corresponding to approximately 0.04 eV/atom higher than the perfect lattice energy. This gentle decrease has been observed in all of our simulations of the atom-exchange effect (see Figs. 6 and 9), and could be attribut-

TABLE III. Results of potential fits to alloys. Here the lattice parameter a is in nm, the atomic volume Ω is in nm^3/atom, and the heat of formation ΔH_f is in eV/atom.

	CuTi		$CuTi_2$		Cu_4Ti_3	
Quantity	Expt. data	Present work	Expt. data	Present work	Expt. data	Present work
a	0.310 8[a]	0.296 1	0.294[a]	0.326 0	0.312 54[c]	0.305 4
Ω	0.014 217[a]	0.014 016	0.015 54[a]	0.013 472	0.013 913[c]	0.013 805
ΔH_f	0.097 4[b]	0.106	0.091 9[b]	0.082 8		0.107 2

[a]Reference 38.
[b]Reference 37.
[c]Reference 43.

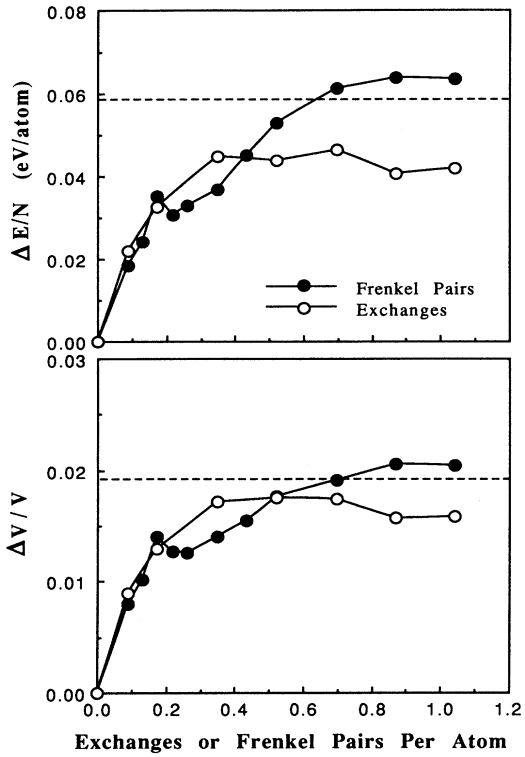

FIG. 2. Changes in the potential energy and volume of a 576-atom CuTi system as functions of the number of atom exchanges or Frenkel pairs. The values calculated for the quenched CuTi liquid are shown by the horizontal dashed lines.

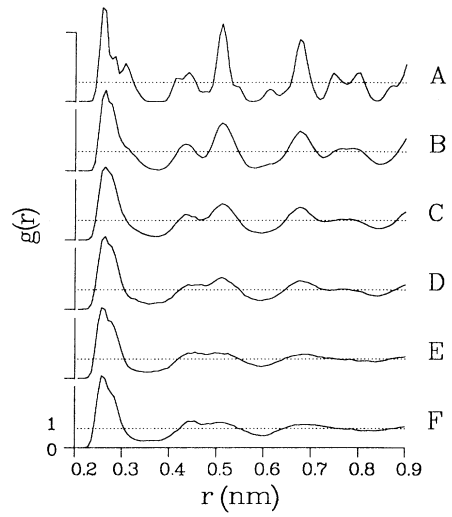

FIG. 3. Pair-correlation functions $g(r)$ of the CuTi compound at 160 K. Curve A is for the perfect lattice. The other curves are for configurations after the following treatments: B, 600 random atom exchanges (1.042 epa); C, 250 Frenkel pairs (0.434 dpa); D, 300 Frenkel pairs (0.521 dpa); E, 400 Frenkel pairs (0.694 dpa); and F, quenched CuTi liquid from 4000 K.

ed to some structural relaxation. The long-range order parameter S, defined as $S=(p-x)/(1-x)$, with p being the probability of finding an A-type atom (A=Cu or Ti) on an ordered lattice site and x the molar fraction of A atoms in the system, was found to be 0.13 and approximately 0 after 300 and 600 exchanges (i.e., 0.521 and 1.042 epa, where epa is exchanges per atom), respectively. The calculated volume expansion is close to the recent experimental value observed at the onset of amorphization in Zr_3Al,[33] and similar to the values obtained for $S \lesssim 0.6$ in $NiZr_2$ by molecular-dynamics simulation.[17] Nevertheless, amorphization was not found after atom exchange in the present work. This is evident in a comparison of $g(r)$ obtained after 600 exchanges (curve B) and $g(r)$ for the perfect lattice (curve A) in Fig. 3, as well as in a comparison of the atom projections onto the (100) plane in Figs. 4(a) and 4(b). Although the random atom exchange has reduced and even eliminated some of the peaks observed for the perfect lattice, a definite structure still remains, indicating that the system was only chemically disordered. It should be noted that the evolution of both the Cu-Cu and Ti-Ti pair-correlation functions (not shown in Fig. 3) is similar to that of the overall $g(r)$.

The effect of nonequilibrium point defects on the volume and potential energy of the equilibrated system is also shown in Fig. 2. It is seen that these quantities first increase rapidly and then slowly approach saturation values which are significantly larger than those obtained by simple atom exchanges. The maximum volume expansion of the lattice, achieved after 500 Frenkel pairs (i.e., 0.868 dpa), is approximately 2.0%, and the corresponding energy increase is approximately 0.06 eV/atom.

The evolution of the structure as the maximum volume and energy are approached is shown by curves C, D, and E in Fig. 3, corresponding to $g(r)$ after the introduction of 250, 300, and 400 Frenkel pairs (i.e., 0.434, 0.521, and

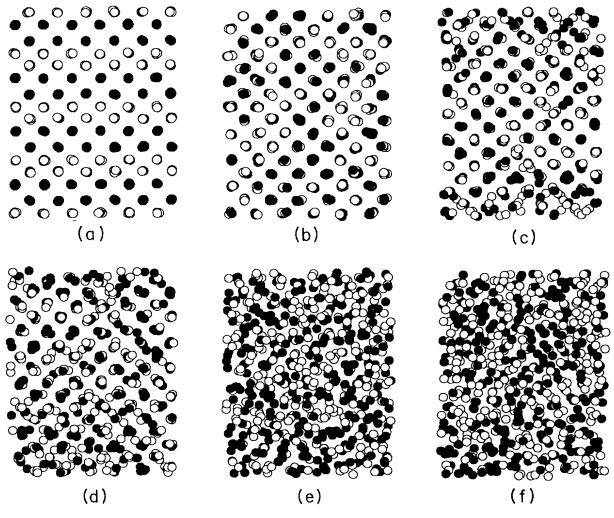

FIG. 4. Projections of atom positions onto the (100) plane in CuTi: (a) for the perfect lattice, (b) after 600 random atom exchanges (1.042 epa), (c) after 250 Frenkel pairs (0.434 dpa), (d) after 300 Frenkel pairs (0.521 dpa), (e) after 400 Frenkel pairs (0.694 dpa), and (f) for the quenched CuTi liquid from 4000 K.

0.694 dpa), respectively. Curve C is similar to curve B with a reduction of peak heights, suggesting that significant chemical disorder is present. Curve D, on the other hand, more closely resembles curve F for the quenched liquid, which shows that amorphization is well under way. Curves E and F are essentially identical, indicating that amorphization is complete. The structural changes can also be visualized by a sequence of (100) atom projections shown in Figs. 4(c)–4(f). The critical damage dose for amorphization (i.e., the damage dose required to complete the amorphization process) can therefore be taken to be approximately 0.7 dpa. The volume expansion at this dose is approximately 1.9%. The calculated volume change and critical damage dose for amorphization are in general agreement with experimental observations.[33,34]

In our previous report on amorphization of CuTi,[16] it was not clear why atom exchange and Frenkel pair introduction had similar effects on volume expansion and energy increase (see Fig. 2). The picture is now clearer with our recent calculations of the stable configurations and energetics of point defects in this compound.[35] In CuTi, the antisite and Frenkel pair formation energies have been calculated to be 0.38 and 2.79 eV, respectively, implying that the introduction of Frenkel pairs should lead to a much greater increase in system energy than the creation of antisite defects. It is seen from Fig. 4(c), however, that most of the Frenkel pairs recombine, apparently resulting in the chemical disorder.

To quantify the differences among the pair-correlation functions $g(r)$ depicted in Fig. 3, we have defined a normalization function G_n, which is a measure of the evolution of $g(r)$ during the c-a transformation. Consider two functions $f_1(r)$ and $f_2(r)$, defined within the interval $[a,b]$. The convolution of these functions over the interval $[a,b]$ is

$$\langle f_1,f_2\rangle_n=\int_a^b f_1(r)f_2(r)r^n dr \ , \tag{9}$$

where the factor r^n may be used to account for, e.g., geometry. Now, if we wish to compare a function $g(r)$ with two functions $p(r)$ and $q(r)$ over the same interval, the normalization function G_n is given by

$$G_n(g;p,q)=\frac{\langle g,p\rangle_n-\langle q,p\rangle_n}{\langle p,p\rangle_n-\langle q,p\rangle_n} \ . \tag{10}$$

In the present work, we used $n=0$, $a=0.2$ nm, $b=0.9$ nm, and the functions p and q were taken to be the pair-correlation functions of the perfect lattice and the quenched system, respectively, at $T=160$ K. For a system having $g(r)$ identical to that of the perfect lattice, $G=1$, whereas for a system with $g(r)$ identical to the quenched system, $G=0$.

In Fig. 5, G is plotted as functions of the number of atom exchanges or Frenkel pairs. It is seen that G decreases monotonically when Frenkel pairs are introduced, reaching zero at a damage dose of 0.7 dpa. With atom exchange alone, G initially decreases at the same rate as with Frenkel pair creation, but bottoms out at a value of approximately 0.5. The plots of G in Fig. 5, as well as the atom projections in Fig. 4, suggest that radiation-induced

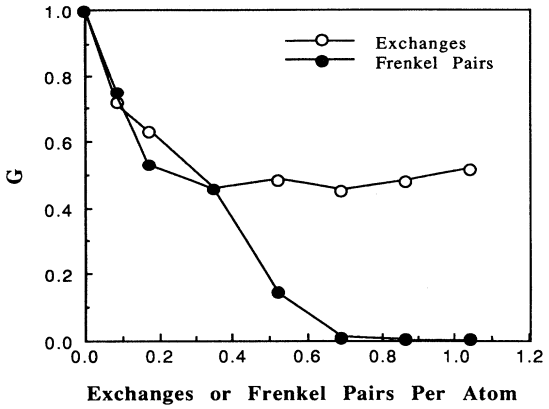

FIG. 5. Plot of G vs the number of atom exchanges or Frenkel pairs normalized to the total number of atoms in the system.

amorphization in CuTi proceeds in the following two-step process: (i) chemical disorder is introduced through point-defect recombination, and then (ii) point defects become stabilized and their populations increase. It is noted that amorphization is only initiated during the second step.

The results of computer simulations by Massobrio, Pontikis, and Martin[17] for amorphization of $NiZr_2$ by chemical disordering are in contradiction with the present study. In their work, only the effects of atom exchange were studied and amorphization was observed for $S \lesssim 0.6$. There are some differences between their work and the present work: different alloys, different interatomic potentials, and different ways of switching atoms. In the present study, atom switching was done rather slowly, allowing enough time between switches for the system to relax somewhat. In the study by Massabrio, Pontikis, and Martin[17] a number of atoms corresponding to a chosen value of S were exchanged simultaneously, and the system was then equilibrated. It is conceivable that this might introduce a large amount of the energy into the system, perhaps shocking it into the amorphous transition. Previous simulation studies have indicated that amorphization depends on defect-introduction rate, even on the time scales accessible to simulations.[14,15] We checked this possibility by performing 500 random exchanges simultaneously and then equilibrating. The result was, however, the same as with the slow rate of switching.

B. Amorphization of $CuTi_2$

Figure 6 summarizes the effects of atom exchange and Frenkel pair introduction the potential energy and volume of an 882-atom $CuTi_2$ system. As the number of exchanges was increased, the energy smoothly increased to a maximum value, which was 0.043 eV/atom higher than that of the perfect lattice, and then slowly decreased. Similarly, the system volume expanded, first reaching a maximum 2.95% higher than the perfect-

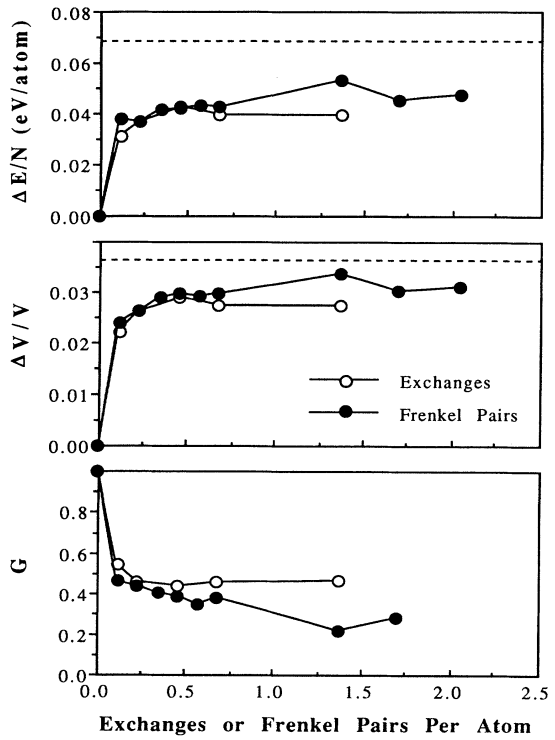

FIG. 6. Changes in the potential energy, volume, and G of an 882-atom $CuTi_2$ system as functions of the number of atom exchanges or Frenkel pairs. The values calculated for the quenched $CuTi_2$ liquid are shown by the horizontal dashed lines.

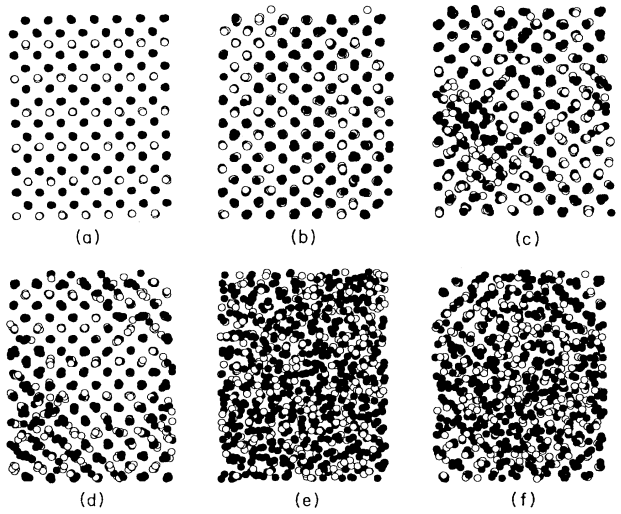

FIG. 7. Projections of atom positions onto the (100) plane of the $CuTi_2$ system: (a) for the perfect lattice; (b) after 1200 random atom exchanges (1.36 epa); (c) after 1200 Frenkel pairs (1.36 dpa); (d) for $G=0.3$, run 1 in Fig. 8; (e) for $G=0$, run 1 in Fig. 8; and (f) for the quenched $CuTi_2$ liquid from 4000 K.

lattice volume after approximately 400 exchanges (i.e., 0.454 epa), and then relaxing to a slightly smaller value. The calculated volume expansion was approximately 50% higher than the result obtained for CuTi. However, as in the case of CuTi, amorphization was not observed after atom exchange in $CuTi_2$. This is evidenced by comparing the (100) atom projections of the perfect lattice and a lattice after 1200 exchanges (i.e., 1.36 epa), shown respectively by Figs. 7(a) and 7(b). Although atom exchange has introduced complete chemical disorder into the lattice, a definite structure still remained.

The overall effect of the Frenkel-pair generation on the $CuTi_2$ system is similar to the effect of random atom exchange, as shown in Fig. 6. A comparison of the pair-correlation functions $g(r)$ (Ref. 36) and the atom projections, Fig. 7(c) with Figs. 7(b) and 7(f), indicates, however, that the system has not become amorphous, even after 1200 Frenkel pairs (i.e., 1.36 dpa); its energy and volume expansion were still below the values calculated for the quenched $CuTi_2$ liquid. This behavior is different from the cases of CuTi and Cu_4Ti_3 (see Sec. III C), and contradicts the experimental observation that $CuTi_2$ can be amorphized by electron irradiation.[9]

Looking at Fig. 6, however, we notice that a larger buildup of defect concentration would be necessary to boost the potential energy to above the quenched-liquid level. This excess buildup was not possible if vacancies and interstitials were produced in pairs in a small volume, due to their mutual recombination. Thus, if, by some means, mutual recombination can be made less efficient, an increase in the defect accumulation will be achieved, which may then trigger the c-a transition. To explore this, we tried different approaches to generate point defects in the system. A simple way to increase the population of defects, either vacancies or interstitials, in our model crystallite, was to introduce them individually, one after the other. The following scheme was chosen to randomly select the order in which the defects were to be created in the system. Consider a system initially consisting N_j atoms of type j, with $\sum_j N_j = N$; let the instantaneous values be n_j, with $\sum_j n_j = n$. Although we expect the total number of atoms n to fluctuate, on the average it should tend toward N. Thus the probability of introducing a vacancy (interstitial) should increase (decrease) with increasing n. In addition, the probability $P_v(n_j)$ of producing a vacancy at a type-j site should be proportional to n_j. These constraints are satisfied if we let

$$P_v(n_j)=\frac{n_j}{2N} . \tag{11}$$

On the other hand, the probability $P_i(n_j)$ of introducing an interstitial of type j should satisfy the conditions $P_i(n_j=N_j)=P_v(n_j=N_j)$ and $\sum_j[P_v(n_j)+P_i(n_j)]=1$, which hold if we let

$$P_i(n_j)=\frac{2N_j-n_j}{2N} . \tag{12}$$

The disadvantage of introducing individual point defects instead of Frenkel pairs is the variability among computer runs because the total number of atoms in the system fluctuates. Consequently, the energy change and volume expansion as a result of point-defect introduction

are not well defined. However, this approach should permit a reasonable simulation of the physical situation, since in reality the vacancies and interstitials are not necessarily present in equal numbers in a given small, local volume of the irradiated specimen, due to, e.g., long-range replacement collision sequences and preferential annihilation of vacancies or interstitials at internal sinks.

The results obtained from three different runs are shown in Fig. 8, where G and $(n-N)/N$ are plotted versus the number of point defects introduced. The positive and negative values of $(n\text{-}N)/N$ correspond to the net accumulation of interstitials and vacancies, respectively, in the system. (Near the onset of amorphization, the concepts of interstitial and vacancy become ill defined; therefore, at this stage, interstitial and vacancy simply mean $n > N$ and $n < N$, respectively.) Generally, in all three runs, G decreased from 1 to 0, indicating that $CuTi_2$ could be amorphized by the production of point defects. Moreover, a correlation between the buildup of interstitial concentration and the amorphization rate was observed. In run 1, for example, as the concentration of interstitials first increased to approximately 5% and then decreased to 0, G dropped steadily, attaining approximately 0 at a damage dose of approximately 0.5 dpa. Two typical (100) atom projections made for $G=0.3$ and 0 are presented in Figs. 7(d) and 7(e). The critical dose for amorphization was found to be larger for a smaller interstitial accumulation. The results of run 3 (Fig. 8) indicated that a strong buildup of vacancies simply led to chemical disordering, with G fluctuating around 0.35, and that the tendency towards amorphization became stronger (i.e., G resumed to decrease to zero) only when there was a net buildup of interstitials.

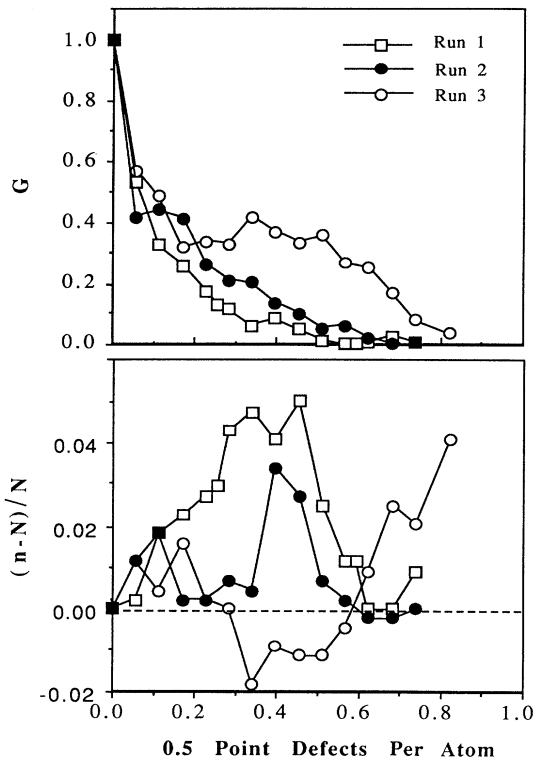

FIG. 8. Plots of G and $(n\text{-}N)/N$ vs the relative number of vacancies and interstitials introduced in the $CuTi_2$ system. Three different runs were carried out.

Another way to increase the effective concentration of interstitials is to introduce several Frenkel pairs simultaneously so as to facilitate interstitial clustering. Indeed, it was found that by simultaneous creation of two Frenkel pairs in each defect-production event, the c-a transition could be triggered.[36] In this case, the onset of amorphization occurred at a damage dose of approximately 0.45 dpa, at which the system volume was expanded by 3.66%.

The present simulation thus shows that $CuTi_2$ can be amorphized by the introduction of point defects, but amorphization occurs only if there exists a large accumulation of interstitials. The fact that the c-a phase transition has been observed in $CuTi_2$ (Ref. 9) would suggest that interstitial clustering is strong and/or the interstitial-vacancy recombination is relatively inefficient in this compound.

Experimentally, Luzzi *et al.*[9] found that amorphization in the ordered $CuTi_2$ undergoing 2-MeV electron irradiation was complete after 0.42 dpa at 183 K and 0.9 dpa and 263 K. Prior to the completion of this transition, the long-range order parameter S decreased rapidly to low values between 0.08 and 0.1. Above a critical temperature of approximately 270 K, amorphization could not be induced. The calculated damage dose for amorphization by introduction of individual point defects at 160 K (approximately 0.5 dpa) is in general agreement with the measurements of Luzzi *et al.*[9]

C. Amorphization of Cu_4Ti_3

The changes in the potential energy, volume, and G of the Cu_4Ti_3 system during atom exchange and introduction of Frenkel pairs are presented in Fig. 9. Similar to the case of CuTi and $CuTi_2$, atom exchanges and Frenkel pairs initially increase the energy and expand the lattice with the same efficiency, because most vacancies and interstitials mutually recombine. After approximately 200 atom exchanges (i.e., 0.397 epa), however, the effect of exchange saturates; after reaching maximum values corresponding to an energy increase of 0.04 eV/atom and a volume expansion of 1.03%, the potential energy and volume decrease slightly to lower values. G decreases rapidly from 1.0 to approximately 0.5 during the first 200 exchanges, and then remains at this level for further atom exchange. On the contrary, after approximately 200 Frenkel pairs, i.e., 0.4 dpa, point defects continue to boost the system energy and volume, which attain maximum values of 0.059 eV/atom and 1.71% at approximately 0.6 dpa, exceeding the quenched-liquid limits of 0.058 eV/atom and 1.65%, respectively. At this dose, G drops to approximately zero, i.e., the c-a transformation is complete. With further introduction of Frenkel pairs, both the energy and volume relax to slightly smaller values, but G is always zero.

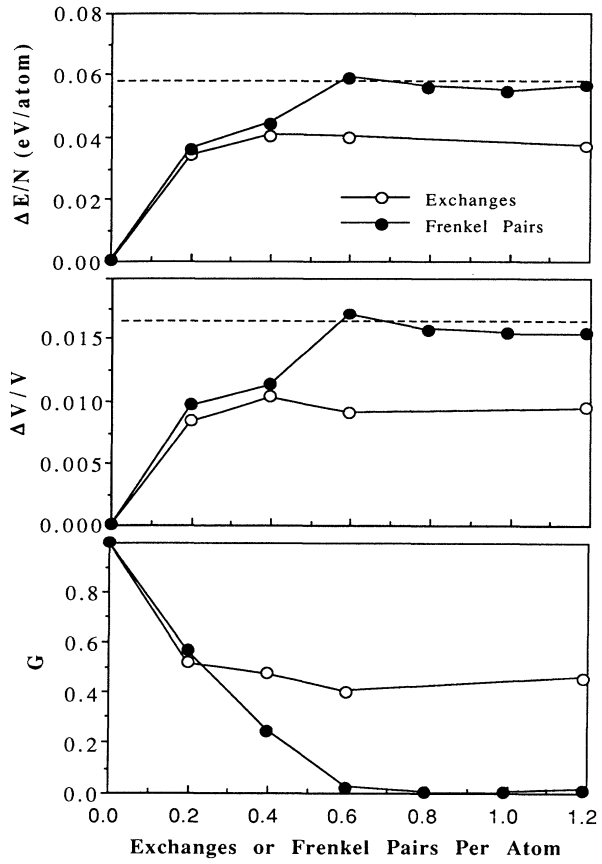

FIG. 9. Potential-energy change, volume expansion, and G of a 504-atom Cu_4Ti_3 system plotted as functions of the normalized number of atom exchanges or Frenkel pairs. The values calculated for the quenched Cu_4Ti_3 liquid are shown by the horizontal dashed lines.

Amorphization of Cu_4Ti_3 by 2-MeV electron irradiation was experimentally investigated by Luzzi *et al.*[10] During irradiation at 175 K, S decreased to 0.26 at a dose of 0.4 dpa, at which the appearance of a faint first halo, signs of amorphization, was noticed. A dose of 0.8 dpa was found necessary to render the irradiated area completely amorphous at this temperature. The results of the present simulations are thus in good accord with these observations.

IV. CONCLUDING REMARKS

In the present computer simulation study, it is found that radiation-induced amorphization of CuTi, $CuTi_2$ and Cu_4Ti_3 occurs as a two-step process: (i) introduction of chemical disorder via point-defect recombination, followed by (ii) stabilization and accumulation of point defects. Although chemical disordering increases the system energy and volume, the *c-a* transition is only initiated during the second step, i.e., the buildup of point defects is a necessary factor for amorphization. The calculated damage doses required to render the ordered compounds amorphous and the volume expansions at the onset of amorphization are in good agreement with the experimental results obtained by Luzzi and Meshii.[3,8–10] However, the findings that atom exchange alone does not cause amorphization conflict with the model proposed by Luzzi and Meshii,[8] who stressed the importance of chemical disordering, based on their observations in electron-irradiated compounds. It is known, nevertheless, that it is impossible in experiments to induce chemical disorder without also generating lattice defects.

Finally, since the introduction of point defects was found to cause amorphization in the three ordered compounds CuTi, $CuTi_2$, and Cu_4Ti_3, one may ask whether lattice defects would also cause pure Cu and Ti to become amorphous. In previous simulation studies, the introduction of point defects resulted in the amorphization of pure systems.[14,15,25] In the present work, the Frenkel pair generation process was repeated on pure 500-atom Cu and 512-atom Ti systems. It was found that even after 500 Frenkel pairs were introduced, the equilibrated systems remained crystalline, in complete agreement with the experimental observation that pure metals cannot be amorphized by irradiation. These observations do not necessarily conflict with the earlier simulation studies, since different simulation temperatures,[25] potentials,[14,15,25] and defect-introduction techniques[14] were used.

ACKNOWLEDGMENTS

The authors would like to thank Dr. P. R. Okamoto and Dr. L. E. Rehn for many stimulating discussions. Part of this work was performed at Argonne National Laboratory. M.J.S. would like to acknowledge the financial support of the Argonne Division of Educational Programs. Support from the Air Force Institute of Technology and the U.S. Department of Energy, Basic Energy Sciences–Materials Sciences, under Contract No. W-31-109-Eng-38, is gratefully acknowledged.

[1]J. L. Brimhall and E. P. Simonen, Nucl. Instrum. Methods B **16**, 187 (1986).
[2]D. F. Pedraza, J. Mater. Res. **1**, 425 (1986); D. F. Pedraza and L. K. Mansur, Nucl. Instrum. Methods B **16**, 203 (1986).
[3]D. E. Luzzi and M. Meshii, Res Mechanica **21**, 207 (1987).
[4]P. R. Okamoto and M. Meshii, in *Science of Advanced Materials,* edited by H. Wiedersich and M. Meshii (American Society for Metals, Metals Park, OH, 1990), p. 33.
[5]J. L. Birmhall, H. E. Kissinger, and L. A. Charlot, Rad. Effects **77**, 237 (1983).
[6]B. Liu, W. L. Johnson, M. A. Nicolet, and S. S. Lau, Nucl. Instrum. Methods **209/210**, 229 (1983).
[7]H. Mori, H. Fujita, M. Tendo, and M. Fujita, Scr. Metall. **18**, 783 (1984).

[8]D. E. Luzzi and M. Meshii, J. Less Common Met. **140**, 193 (1988).
[9]D. E. Luzzi, H. Mori, H. Fujita, and M. Meshii, Mater. Res. Soc. Symp. Proc. **51**, 479 (1985).
[10]D. E. Luzzi, H. Mori, H. Fujita, and M. Meshii, Acta Metall. **34**, 629 (1986).
[11]H. Mori, H. Fujita, and M. Fujita, Jpn. J. Appl. Phys. **22**, L94 (1983).
[12]Y. Limoge and A. Barbu, Phys. Rev. B **30**, 2212 (1984).
[13]E. P. Simonen, Nucl. Instrum. Methods B **16**, 198 (1986).
[14]H. Hsieh and S. Yip, Phys. Rev. Lett. **59**, 2760 (1987).
[15]Y. Limoge, A. Rahman, H. Hsieh, and S. Yip, J. Non-Cryst. Solids **99**, 75 (1988).
[16]M. J. Sabochick and N. Q. Lam, Scr. Metall. Mater. **24**, 565 (1990).
[17]C. Massobrio, V. Pontikis, and G. Martin, Phys. Rev. Lett. **62**, 1142 (1989); Phys. Rev. B **41**, 10 486 (1990).
[18]M. L. Swanson, J. R. Parsons, and C. W. Hoelke, Rad. Effects **9**, 249 (1971).
[19]D. Beretz, J. Hillairet, and M. Halbwachs, J. Phys. (Paris) Colloq. **42**, C10-747 (1981).
[20]J. P. Riviere and J. Grilhe, Acta Metall. **20**, 1275 (1972).
[21]J. P. Riviere, H. Zonon, and J. Grilhe, Acta Metall. **22**, 929 (1974).
[22]O. Dimitrov and C. Dimitrov, J. Nucl. Mater. **105**, 39 (1982).
[23]E. P. Simonen, Nucl. Instrum. Methods B **16**, 198 (1986).
[24]A. T. Motta, D. R. Olander, and A. J. Machiels, in *Effects of Radiation on Materials,* Proceedings of the 14th International Symposium of the American Society for Testing and Materials, STP 1046, edited by N. H. Packan, R. E. Stoller, and A. S. Kumar (American Society for Testing and Materials, Philadelphia, 1989), Vol. I, p. 457.
[25]K. Maeda and S. Takeuchi, Philos. Mag. B **52**, 955 (1985).
[26]H. Hsieh and S. Yip, Phys. Rev. B **39**, 7476 (1989).
[27]M. S. Daw, M. I. Baskes, and S. M. Foiles (private communication).
[28]M. S. Daw and M. I. Baskes, Phys. Rev. B **29**, 6443 (1984).
[29]M. J. Sabochick and S. Yip, J. Phys. F **18**, 1689 (1988).
[30]D. J. Oh and R. A. Johnson, J. Mater. Res. **3**, 471 (1988).
[31]S. P. Chen, A. F. Voter, R. C. Albers, A. M. Boring, and P. J. Hay, J. Mater. Res. **5**, 955 (1990).
[32]J. H. Rose, J. R. Smith, F. Guinea, and J. Ferrante, Phys. Rev. B **29**, 2963 (1984).
[33]P. R. Okamoto, L. E. Rehn, J. Pearson, R. Bhadra, and M. Grimsditch, J. Less Common Met. **140**, 231 (1988).
[34]J. Koike, P. R. Okamoto, L. E. Rehn, and M. Meshii, J. Mater. Res. **4**, 1143 (1989).
[35]J. R. Shoemaker, R. T. Lutton, D. Wesley, W. R. Wharton, M. L. Oehrli, M. S. Herte, M. J. Sabochick, and N. Q. Lam, J. Mater. Res. (to be published).
[36]M. J. Sabochick and N. Q. Lam, Mater. Res. Soc. Symp. Proc. (to be published).
[37]M. Arita, R. Kinaka, and M. Someno, Met. Trans. **10A**, 529 (1979).
[38]*Structure Reports,* edited by A. J. C. Wilson (International Union of Crystallography, Utrecht, 1951), Vol 15, p. 69.
[39]G. Simmons and H. Wang, *Single Crystal Elastic Constants and Calculated Aggregate Properties: A Handbook* (Massachusetts Institute of Technology, Cambridge, MA, 1971).
[40]R. W. Siegel, in *Positron Annihilation,* edited by P. G. Coleman, S. C. Sharma, and L. M. Diana (North-Holland, Amsterdam, 1982), p. 351.
[41]T. Gorecki, Z. Metallkde. **65**, 426 (1974).
[42]C. Kittel, *Introduction to Solid State Physics,* 4th ed. (Wiley, New York, 1971).
[43]D. E. Luzzi and M. Meshii, J. Mater. Res. **1**, 617 (1986).